Energetic and Structural Consequences of Desolvation/Solvation Barriers to Protein Folding/Unfolding Assessed from Experimental Unfolding Rates

David Rodriguez-Larrea, Beatriz Ibarra-Molero, and Jose M. Sanchez-Ruiz
Facultad de Ciencias, Departamento de Quimica Fisica, 18071-Granada, Spain

ABSTRACT Theoretical work has suggested the existence of solvation/desolvation barriers in protein folding/unfolding processes. We propose that the energetic and structural consequences of such barriers for the folding transition state can be assessed from experimental unfolding rates using well-established structure-energetics relationships. For a set of proteins of size within the 60–130 number-of-residues range, we find energetic effects associated to solvation/desolvation on the order of 10^2 kJ/mol. This supports that the folding transition states may be characterized by large networks of water-unsatisfied, broken internal contacts. In terms of buried surface, we estimate the typical network size to be on the order of several thousands of $Å^2$, or ~50% of the total change in accessible surface area upon unfolding. The analyses reported here thus suggest a clear structural picture for the different energetic balance of native and folding transition states.

Received for publication 27 April 2006 and in final form 19 June 2006.

Address reprint requests and inquiries to Jose M. Sanchez-Ruiz, Tel.: 34-958-243-189; E-mail: sanchezr@ugr.es.

Theoretical work has suggested the existence of enthalpic (energetic) desolvation barriers in at least some protein folding processes (1,2). In simple terms, such barriers are associated to the asynchrony between water escape and formation of internal interactions. Accordingly, the transition state would be characterized by a network of water-unsatisfied, broken internal contacts (see Fig. 1 for a pictorial illustration). In fact, desolvation has been suggested as the likely origin of the robust enthalpic barriers detected by Chevron-Eyring analysis of protein folding rates (3,4).

It must be noted that, when considered from a protein unfolding viewpoint, the barrier could be viewed as arising from the asynchrony between water penetration and the breaking of internal interactions and would be described as a ''solvation'' barrier (see Fig. 1). We show here that the energetic and structural consequences of solvation barriers for the folding transition state can be estimated from experimental unfolding rates using well-known structure-energetics correlations.

The enthalpy change associated to a protein conformational change includes contributions from breaking/formation of internal interactions (ΔH_{int}) and from the hydration/dehydration of the residues that become exposed-to-solvent/buried (5):

$$\Delta H = \Delta H_{\mathrm{int}} + \Delta H_{\mathrm{hyd}}. \tag{1}$$

For the conversion of the native to the unfolded state (*N* and *U* in Fig. 1), both contributions are linked (i.e., breaking of the internal interactions involving given residues implies the exposure of those residues to the solvent). In addition, both contributions have been shown to scale with changes in accessible surface area (5). Consequently, experimental enthalpy changes for protein unfolding have been shown to be well represented by the following empirical parametrization in terms of the unfolding changes in polar and apolar ASA:

$$\Delta H_{\mathrm{N\rightarrow U}} = a \cdot \Delta\mathrm{ASA}_{\mathrm{pol}} + b \cdot \Delta\mathrm{ASA}_{\mathrm{ap}}, \tag{2}$$

where $a = -101.2\ \mathrm{J{\cdot}mol^{-1}{\cdot}Å^{-2}}$ and $b = 169.5\ \mathrm{J{\cdot}mol^{-1}{\cdot}Å^{-2}}$ for $T = 25°\mathrm{C}$ (6). Since native proteins bury an approximately constant proportion of polar and apolar ASA upon folding (0.417 ± 3.4% and 0.583 ± 3.4%, respectively, as reported in Robertson and Murphy (7), Eq. 2 can be easily expressed in terms of the total unfolding ASA change:

$$\Delta H_{\mathrm{N\rightarrow U}} = \alpha \cdot \Delta\mathrm{ASA}_{\mathrm{N\rightarrow U}}, \tag{3}$$

where $\alpha = 11.7\ \mathrm{J{\cdot}mol^{-1}{\cdot}Å^{-2}}$ for $T = 25°\mathrm{C}$.

Consider now the unfolding activation energy. $\Delta H_{\mathrm{N\rightarrow TS}}$ has contributions associated to the surface exposed to the solvent upon formation of the transition state from the native protein (the *blue* surface in Fig. 1) and to the residues with broken internal interactions but not yet exposed to the solvent (the *red* surface in Fig. 1) . The former contribution reflects compensated internal interactions and hydration terms (as in the global unfolding process) and, therefore, can be estimated from Eq. 3 with the activation change in ASA. The latter contribution (ΔH^*) is the enthalpic term associated to the solvation barrier we actually seek to calculate. Accordingly, the activation enthalpy can be written as

© 2006 by the Biophysical Society
doi: 10.1529/biophysj.106.087932

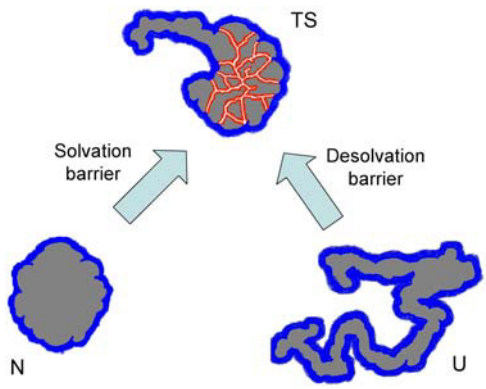

FIGURE 1 Pictorial illustration of desolvation/solvation barriers to protein folding/unfolding. The surface shown in blue in the native (*N*), unfolded (*U*), and transition (*TS*) states is exposed to the solvent. The surface shown in red in the transition state represents broken internal contacts, which are not solvated by water.

$$\Delta H_{N\to TS} = \Delta H^* + \alpha \cdot \Delta ASA_{N\to TS}. \quad (4)$$

Values of $\Delta H_{N\to TS}$ are experimentally available as activation energies for the unfolding process. Provided that some estimate is available for the activation change in ASA, Eq. 4 can be solved for ΔH^*. $\Delta ASA_{N\to TS}$ can be readily estimated from kinetic, denaturant *m* values, since denaturant *m* values are proportional to changes in surface exposed to the solvent (8).

The kind of calculation we have just outlined can be illustrated with the experimental data for hen egg white lysozyme unfolding reported in Ibarra-Molero and Sanchez-Ruiz (9). Fig. 2 shows Arrhenius plots for lysozyme unfolding rates at several high guanidine concentrations. These plots are essentially linear, supporting that the activation energy values can be taken as temperature-independent within the temperature range of the experimental data (18–45°C). They do depend somewhat on guanidine concentration, but the dependence appears linear (*inset* in Fig. 2) and allows the $\Delta H_{N\to TS}$ value to be obtained as an extrapolation to zero denaturant concentration. We take the value thus obtained (208 kJ/mol) to be valid at 25°C. Under the assumption that denaturant *m* values and ASA values are linearly related (8), $\Delta ASA_{N\to TS}$ is given by $\Delta ASA_{N\to U}\cdot(m_{N\to TS}/m_{N\to U})$. $\Delta ASA_{N\to U}$ for lysozyme unfolding is calculated as 14978 Å^2 (10) and, from Ibarra-Molero and Sanchez-Ruiz (9), the kinetic and equilibrium *m* values are 2.9 and 10.5 kJ·mol^{-1}·M^{-1}. Then, $\Delta ASA_{N\to TS}$ is estimated as 4090 Å^2 (11) and the $\alpha\cdot\Delta ASA_{N\to TS}$ term in Eq. 4 is 48 kJ/mol, significantly smaller than the experimental $\Delta H_{N\to TS}$ value (208 kJ). The difference gives a large ΔH^* value of 160 kJ/mol. This result is qualitatively robust; for instance, modifying the value of α (Eqs. 3 and 4) by as much as plus/minus 50% only results in a change of ~30 kJ/mol in the calculated ΔH^* value. It must be noted, in addition, that we have used a tripeptides model to calculate the ASA of the unfolded state (10); use of more compact models (12) would lead to even higher estimates of ΔH^*.

We have carried out the above calculation with other protein systems for which the required experimental data are available in the literature (see Supplementary Material for details). The outcome of these calculations is summarized in Fig. 3 *A* as plots of ΔH^* and $\alpha\cdot\Delta ASA_{N\to TS}$ (the two contributions to the activation energy according to Eq. 4) versus $\Delta H_{N\to TS}$. In all cases, large values of ΔH^* are found. In fact, the values of the slopes of the plots in Fig. 3 *A* indicate that, for the protein set studied, ~80% of the activation energy value is to be attributed to the solvation barrier. A measure of the structural impact of such solvation barriers can be derived from the ΔH^* values using the following equation:

$$\Delta H^* = \beta_{ap}\cdot U_{ap}^6\cdot ASA_{ap}^* + \beta_{pol}\cdot U_{pol}^6\cdot ASA_{pol}^* + \beta_{mix}\cdot U_{mix}^6\cdot ASA^*, \quad (5)$$

which is based upon the parametrization of the enthalpy changes for breaking of internal interactions reported by Freire and co-workers (5). Equation 5 takes into account the apolar-apolar, polar-polar, and polar-apolar (i.e., ''mix'') internal interactions and the *U* parameters are the corresponding energy-averaged separation distances. The *U* values are always close to 0.73 (see Table I in Hilser et al. (5)); using this, the values of β_{ap}, β_{pol}, and β_{mix} given in Hilser et al. (5), and the known fractions of polar and apolar surface buried upon folding (0.417 ± 3.4% and 0.583 ± 3.4%, respectively, as reported in Robertson and Murphy (7)), Eq. 5 can be simplified to

$$ASA^* \approx \Delta H^*/\beta \quad (6)$$

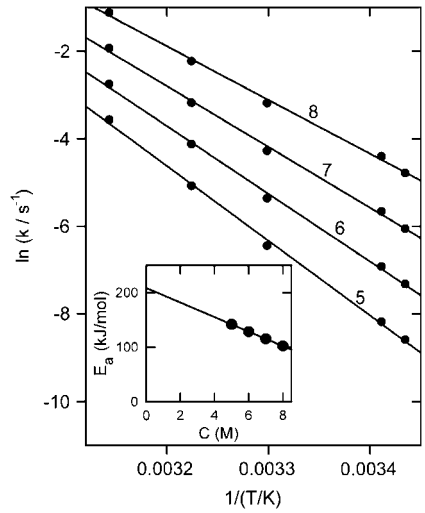

FIGURE 2 Arrhenius plots for hen egg white lysozyme unfolding at several guanidine concentrations (numbers alongside the lines). The inset shows a plot of activation energy versus guanidine concentration; extrapolation to zero denaturant concentration yields the activation energy in water ($\Delta H_{N\to TS}$ = 208 kJ/mol).

with $\beta = 24\ \mathrm{J{\cdot}mol^{-1}{\cdot}\AA^{-2}}$. As shown in Fig. 3 *B*, the ASA* values thus estimated are surprisingly large: on the order of several thousands of Å^2. This suggests that the broken, water-unsatisfied contacts may form large, extended networks in the transition states for protein folding/unfolding. In fact, the slopes of the plots of $\Delta ASA_{N\rightarrow TS}$ and ASA* versus $\Delta ASA_{N\rightarrow U}$ of Fig. 3 *B* indicate that, for the protein set studied, ~30% of the total unfolding ASA change is already exposed to the solvent in the transition state and ~50% of that total ASA change is still buried but involved in broken internal contacts.

The analyses reported here focus on the energetic (enthalpic) consequences of solvation/desolvation barriers. Certainly, enthalpy is only half of the story, since the free energy associated to these barriers will have enthalpic as well as entropic components (4,13). Nevertheless, the analysis of activation enthalpies according to known structure-energetics relationships reveals the different energetic balance of the native and folding transition states and provides a clear qualitative picture of the structural consequences of solvation/desolvation for the transition states.

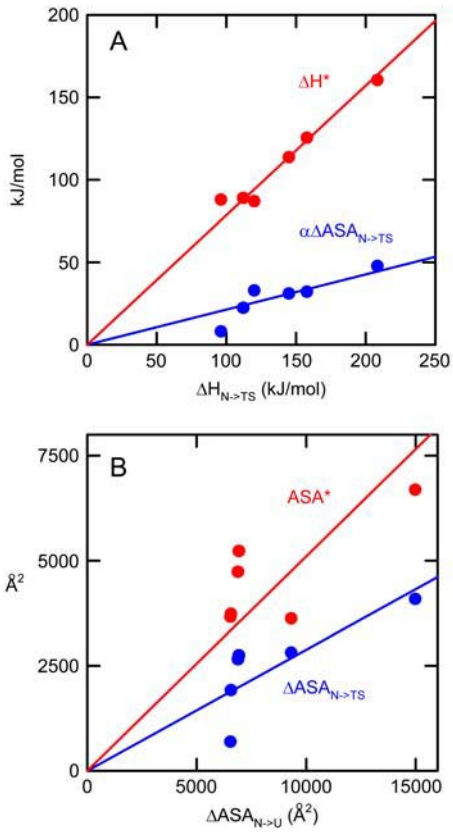

FIGURE 3 Energetic (panel *A*) and structural (panel *B*) consequences of the solvation barrier for the unfolding transition state for the following proteins: hen egg white lysozyme, chymotrypsin inhibitor 2, apocytochrome B_5, cold shock protein B (from *Bacillus subtilis*), coiled-coil peptide GCN4-p1, and IgG binding domain of protein L.

SUPPLEMENTARY MATERIAL

An online supplement to this article can be found by visiting BJ Online at http://www.biophysj.org.

ACKNOWLEDGMENTS

This work was supported by grant BIO2003-02229 from the Spanish Ministry of Science and Education, Feder Funds, and grant CVI-0771 from the ''Junta de Andalucía''.

REFERENCES and FOOTNOTES

1. Rank, J. A., and D. Baker. 1997. A desolvation barrier to hydrophobic cluster formation may contribute to the rate-limiting step in protein folding. *Protein Sci.* 6:347–354.
2. Cheung, S. M., A. E. Garcia, and J. N. Onuchic. 2002. Protein folding mediated by solvation: water expulsion and formation of the hydrophobic core occur after the structural collapse. *Proc. Natl. Acad. Sci. USA.* 99:685–690.
3. Scalley, M. L., and D. Baker. 1997. Protein folding kinetics exhibits an Arrhenius temperature dependence when corrected for the temperature-dependence of protein stability. *Proc. Natl. Acad. Sci. USA.* 94:10636–10640.
4. Liu, Z., and H. S. Chan. 2005. Desolvation is a likely origin of robust enthalpic barriers to protein folding. *J. Mol. Biol.* 349:872–889.
5. Hilser, V. J., J. Gomez, and E. Freire. 1996. The enthalpy change in protein folding and binding: refinement of parameters for structure-based calculations. *Proteins.* 26:123–133.
6. These values at 25 °C are easily calculated from the reported values at the reference temperature of 60 °C (5), taking into account that the polar and apolar contributions to the unfolding enthalpy change with temperature according to the corresponding contributions to the unfolding heat capacity.
7. Robertson, A. D., and K. P. Murphy. 1997. Protein structure and the energetics of protein stability. *Chem. Rev.* 97:1251–1267.
8. Myers, J. K., C. N. Pace, and J. M. Scholtz. 1995. Denaturant *m* values and heat capacity changes: relation to changes in accessible surface areas of protein unfolding. *Protein Sci.* 4:2138–2148.
9. Ibarra-Molero, B., and J. M. Sanchez-Ruiz. 1996. A model-independent, nonlinear extrapolation procedure for the characterization of protein folding energetics from solvent-denaturation data. *Biochemistry.* 35:14689–14702.
10. ASA values for the native states where calculated using a modification of the Shrake-Rupley algorithm, which randomly places 2000 points in the expanded van der Waals sphere representing each atom. A radius of 1.4 Å for the solvent probe and Chothia set for the protein atoms were used. ASA values for the unfolded states were calculated on the basis of a Gly-X-Gly tripeptides model.
11. Alternatively, $\Delta ASA_{N\rightarrow TS}$ could be calculated solely from the kinetic *m* value by using the slope of the plot of guanidine-m versus ASA reported in Hilser et al. (5) (0.92 $\mathrm{J{\cdot}mol^{-1}{\cdot}M^{-1}{\cdot}\AA^{-2}}$). The result obtained (3117 Å^2), however, is close to that calculated using the method described in the text (4089 Å^2) and the difference would not significantly modify the ΔH^* value (from 160 kJ/mol to 172 kJ/mol) and the subsequent interpretations.
12. Ibarra-Molero, B., I. M. Plaza del Pino, B. Souhail, H. O. Hammou, and J. M. Sanchez-Ruiz. 2000. The sarcosine effect on protein stability: a case of nonadditivity? *Protein Sci.* 9:820–826.
13. Solvent entropy (4) and side-chain conformational entropy of the residues involved in broken internal interactions are among the likely contributors to the solvation activation entropy. However, estimation of $\Delta S_{N\rightarrow TS}$ from experimental unfolding rates within the framework of transition-state theory is hampered by uncertainties associated with the value of the front factor in the Eyring equation. In any case, due to enthalpy-entropy compensation, a low free-energy barrier can be consistent with a high enthalpic solvation/desolvation barrier, as Liu and Chan have pointed out (4). In fact, the solvation/desolvation free-energy barrier is expected to vanish in cases of downhill folding.